# Synthesis and Characterization of Mesostructured Titania-Based Materials Through Evaporation-Induced Self-Assembly

**ARTICLE** *in* CHEMISTRY OF MATERIALS · JANUARY 2002

Impact Factor: 8.35 · DOI: 10.1021/cm011217a



**3 AUTHORS**, INCLUDING:

Galo J A A Soler-Illia
National University of General San Martín
**144** PUBLICATIONS **8,193** CITATIONS

SEE PROFILE

Clément Sanchez
college DE france , Pierre and Marie Curie Uni…
**600** PUBLICATIONS **25,666** CITATIONS

SEE PROFILE

# Synthesis and Characterization of Mesostructured Titania-Based Materials through Evaporation-Induced Self-Assembly

G. J. de A. A. Soler-Illia, A. Louis, and C. Sanchez*

*Chimie de la Matière Condensée, UMR CNRS 7574, Université Pierre et Marie Curie, 4 place Jussieu, 75252 Paris, France*

*Received August 7, 2001. Revised Manuscript Received October 30, 2001*

Mesostructured $TiO_2$−hexadecyltrimethylammonium bromide hybrid powders, displaying a bidimensional hexagonal pattern (p6m), have been synthesized by an evaporation-induced self-assembly (EISA) method, in ethanol/HCl/$H_2O$ media. Thermal treatment of these "titaniatropic" hybrid phases leads to phosphorus-free, high surface area (280−370 $m^2\ g^{-1}$) mesoporous titania, with 20−25 Å pores. The role of the synthesis parameters (surfactant and acid concentrations and temperature) is thoroughly discussed to understand their influence on the hybrid mesostructures. It is suggested that hydrophilic Ti-oxo nanometric building blocks formed in the acidic synthesis conditions self-assembly upon solvent evaporation to produce organized structures.

## Introduction

Mesostructured and mesoporous materials have attracted a great deal of attention since the discovery of the M41S family by scientists of Mobil Oil.[1] All synthesis methods subsequently described opened the way to the field of Chemistry of Organized Matter,[2] where a successful union between *sol−gel chemistry* and *self-assembly* permits one to obtain supramolecularly templated materials, which present arrays of organized pores of tailored dimensions and a great variety of shapes.[3,4]

The preparation of mesoporous silica is nowadays widespread; a great range of structures can be obtained,[5] and the basic features of the processes involved in the formation of these phases are beginning to be understood.[6−8] In comparison, mesoporous transition-metal (TM)-based materials have been less explored, despite the enormous potential of TM-based mesoporous oxides.[5a,9−11] The main obstacle to obtain these phases is the higher reactivity of M(IV) toward condensation compared to Si(IV). Therefore, a careful tuning of the sol−gel chemistry and the self-assembly processes is essential.

In particular, high surface area mesostructured $TiO_2$ is a very interesting material, in view of controlled delivery, catalytic, photocatalytic, or energy conversion applications.[12] Most of the proposed syntheses of mesoporous titania or titanium phosphates by precipitation rely on controlling the high reactivity of Ti(IV) by the addition of stabilizing agents. Indeed, uncontrolled hydrolysis and condensation lead to the rapid formation of a dense inorganic network, generating poorly structured materials. The use of complex $Ti(OR)_{4-n}(acac)_n$ (acac = acetylacetonate) precursors, combined with phosphonate anionic surfactants in slightly acid medium (pH 3−6), led to the first documented titania-based mesoporous oxide, TMS-1.[13] Besides the fact that TMS-1 has been a matter of debate,[14,15] the underlying idea is valid, and other organic bidentate ligands have been used.[16] A tridentate ligand, triethanolamine, allows the production of phosphorus-free wormlike, mesoporous $TiO_2$.[17] This method has been extended to other metal and nonmetal centers.[18] Recently, hydrogen peroxide

* To whom correspondence should be addressed. E-mail: clems@ccr.jussieu.fr.

(1) (a) Kresge, C. T.; Leonowicz, M. E.; Roth, W. J.; Vartuli, J. C.; Beck, J. S. *Nature* **1992**, *359*, 710. (b) Beck, J. S.; Vartuli, J. C.; Roth, W. J.; Leonowicz, M. E.; Kresge, C. T.; Schmitt, K. D.; Chu, C. T.-W.; Olson, D. H.; Sheppard, E. W.; McCullen, S. B.; Higgins, J. B.; Schlenker, J. L. *J. Am. Chem. Soc.* **1992**, *114*, 10834. (c) Beck, J. S.; Vartuli, J. C. *Curr. Opin. Solid State Mater. Sci.* **1996**, *1*, 76.

(2) Mann, S.; Burkett, S. L.; Davis, S. A.; Fowler, C. E.; Mendelson, N. H.; Sims, S. D.; Walsh, D.; Whilton, N. T. *Chem. Mater.* **1997**, *9*, 2300.

(3) Mann, S.; Ozin, G. A. *Nature* **1996**, *382*, 313.

(4) Ozin, G. A. *Chem. Commun.* **2000**, 419.

(5) Recent reviews on this subject include (a) Ying, J. Y.; Mehnert, C.; Wong, M. S. *Angew. Chem., Int. Ed. Engl.* **1999**, *38*, 57. (b) Barton, T. J.; Bull, L. M.; Klemperer, W. G.; Loy, D. A.; McEnaney, B.; Misono, M.; Monson, P. A.; Pez, G.; Scherer, G. W.; Vartuli, J. C.; Yaghi, O. M. *Chem. Mater.* **1999**, *11*, 2633. (c) Zhao, D.; Yang, P.; Huo, Q.; Chmelka, B. F.; Stucky, G. D. *Curr. Opin. Solid State Mater. Sci.* **1998**, *3*, 111. (d) Göltner, C. G.; Antonietti, M. *Adv. Mater.* **1997**, *9*, 431.

(6) Monnier, A.; Schüth, F.; Huo, Q.; Kumar, D.; Margolese, D.; Maxwell, R. S.; Stucky, G. D.; Krishnamurty, M.; Petroff, P.; Firouzi, A.; Janicke, M.; Chmelka, B. F. *Science* **1993**, *261*, 1299.

(7) Huo, Q.; Margolese, D. I.; Ciesla, U.; Demuth, D. G.; Feng, P.; Gier, T. E.; Sieger, P.; Firouzi, A.; Chmelka, B. F.; Schüth, F.; Stucky, G. D. *Chem. Mater.* **1994**, *6*, 1176.

(8) Tolbert, S. H.; Landry, C. C.; Stucky, G. D.; Chmelka, B. F.; Norby, P.; Hanson, J. C.; Monnier, A. *Chem. Mater.* **2001**, *13*, 2247 and references therein.

(9) Behrens, P. *Angew. Chem., Int. Engl. Ed.* **1996**, *35*, 515.

(10) Sayari, A.; Liu, P. *Microporous Mater.* **1997**, *12*, 149.

(11) Schüth, F. *Chem. Mater.* **2001**, *13*, 3184.

(12) Hagfeldt, A.; Grätzel, M. *Chem. Rev.* **1995**, *95*, 45.

(13) Antonelli, D. M.; Ying, J. Y. *Angew. Chem., Int. Ed. Engl.* **1995**, *34*, 2014.

(14) Putnam, R. L.; Nakagawa, N.; McGrath, K. M.; Yao, N.; Aksay, I. A.; Gruner S. M.; Navrotsky, A. *Chem. Mater.* **1997**, *9*, 2690.

(15) Stone, V. F., Jr.; Davis, R. J. *Chem. Mater.* **1998**, *10*, 1468.

(16) Fröba, M.; Muth, O.; Reller, A. *Solid State Ionics* **1997**, *101−103*, 249.

(17) Cabrera, S.; El-Haskouri, J.; Beltrán-Portier, A.; Beltrán-Portier, D.; Marcos, M. D.; Amorós, P. *Solid State Sci.* **2000**, *2*, 513.

10.1021/cm011217a CCC: $22.00 
Published on Web 01/11/2002

was used as a hydrolysis−condensation inhibitor in basic media, leading to mesoporous $TiO_2$.[19] In acid media, protons have been used to retard rapid condensation and generate titanium mesostructured oxosulfates[20] or mesoporous oxophosphates.[21] The use of nonaqueous solvents combined with complexing agents has also been explored.[22] Nonionic amine templates have been applied to avoid phosphate pollution, leading to wormlike phases.[23] A wormlike material is also obtained by resorting to ultrasonic irradiation, to shorten the reaction times.[24]

The so-called evaporation-induced self-assembly (EISA) process is an alternative synthetic approach that allows the tuning of inorganic condensation with the formation of a mesoorganized liquid-crystal template.[25] As solvent is removed, a mesophase is gradually formed. The accumulation of inorganic material around the voids of this liquid-crystalline phase allows one to obtain well-defined mesostructured hybrids, which present a segregation of organic and mineral domains at the nanoscale. This procedure also allows processing of the macroscopic shape of the material (aerosol, powder, monoliths, and films). The hybrid structure is quite flexible as-synthesized, because of incomplete inorganic polymerization. A subsequent "locking" step is necessary, enhancing inorganic polymerization in order to obtain a robust mesostructure. This is an interesting procedure for TM-based materials, because starting solutions are relatively dilute, and the inorganic polymerization can be readily controlled by an acid, which is subsequently eliminated by evaporation. Stucky's group was the first to apply this route for many TM oxides (Ti, Zr, ...) by using ethanolic solutions of $MCl_n$ and triblock copolymers as templates.[26,27] Selective alcohol evaporation favors the gradual formation of an organized lyotropic phase, and the inorganic framework is formed around the micelles. In the first interpretation, a nonhydrolytic condensation path was considered to be responsible for the formation of the mineral framework. However, in the reported synthesis conditions, ordinary condensation must prevail, with water being provided by moisture or impurities, as shown by further detailed studies in alkoxide/alcohol/water/HCl mixtures.[28,29] Moreover, studies on these and related systems (precursor solutions,[28] "bulk" gels or powders,[29] or thin films[30]) stress the role of water in the mesoscopic organization. In addition, the use of preformed hydrophobic clusters to generate mesostructured $TiO_2$ in low-water conditions results in wormlike structures.[31] Actual nonhydrolytic conditions (absence of water; $T > 150$ °C) have been recently used to synthesize high surface area wormlike mesoporous mixed oxides.[32]

**Table 1. Synthetic Conditions of $TiO_2$/CTAB Hybrid Mesophases[a]**

| condition | $T$ (°C) | aging time (days) | TET | CTAB | HCl | $H_2O$ | EtOH |
|---|---|---|---|---|---|---|---|
| Ti-A-100-$sT$ | 25−70 | 7 | 1 | 0.08−0.4 | 1.4 | 17 | 20 |
| Ti-B-45-$pT$ | 25−70 | 10 | 1 | 0.2 | 1.4−10 | 45 | 70 |
| Ti-B-90-$pT$ | 25−70 | 10 | 1 | 0.2 | 1.4−10 | 90 | 70 |

[a] $s$ = [CTAB]/[Ti]; $h$ = [$H_2O$]/[Ti]; $p$ = [HCl]/[Ti].

In this work, we apply an EISA method to synthesize hybrid titania-based materials in an easy and reproducible way. The hybrids present different mesostructures: bicontinuous wormlike or bidimensional hexagonal amorphous titania. The hybrid materials are "titaniatropic" (i.e., hybrid liquid-crystalline phases; cf. ref 33), flexible mesostructures that are only partially condensed. These mesostructured phases are composed of preformed titania nanobuilding blocks (NBB), which are self-assembled within a liquid-crystal-like mesophase, around micellar assemblies. This mesostructure is thermally reinforced, to assist inter-NBB condensation, leading to robust hybrid precursors. Thermal treatment of these precursors leads to high surface area phosphate-free $TiO_2$ that presents organized porosity in the frontier of the micro- and mesoporous domains. This material presents interesting features: the pore surface is large and accessible, and the chemical nature of the walls should permit their subsequent functionalization, leading to an ordered multifunctional material, where the wall nature, interface, and pore interior can be subsequently tailored.

## Experimental Section

Titanium ethoxide, TET ($Ti(O-CH_2CH_3)_4$; 99%, Fluka), was used as the metal source, and hexadecyltrimethylammonium bromide (CTAB; Aldrich) was employed as the template. HCl (Carlo Erba p.a. reagent) was used as a condensation inhibitor. Solutions were made up using mixtures of absolute ethanol, pure HCl, and deionized water.

In a typical synthesis, an inorganic solid is formed by dropwise addition of TET in an ethanolic HCl solution with vigorous stirring until total dissolution of any solid (2 h at ambient temperature; less than 20 min at 60 °C) was reached. To this solution, an ethanolic solution of the surfactant is added. In all cases, the surfactant-to-metal ratios ($s$ = [CTAB]/[Ti]) were between 0.1 and 0.4; the nominal hydrolysis ratio ($h = H_2O/Ti$) was set up between 17 and 90; the HCl/Ti ratio ($p$) varied between 0 and 10. Table 1 summarizes the explored conditions (i.e., Ti-A and Ti-B) which gave rise to organized hybrid phases.

(18) Cabrera, S.; El-Haskouri, J.; Guillem, C.; LaTorre, J.; Beltrán-Portier, A.; Beltrán-Portier, D.; Marcos, M. D.; Amorós, P. *Solid State Sci.* **2000**, *2*, 405 and references therein.
(19) Trong On, D. *Langmuir* **1999**, *15*, 8561.
(20) Lindén, M.; Blanchard, J.; Schacht, S.; Schunk, S.; Schüth, F. *Chem. Mater.* **1999**, *11*, 3002.
(21) Blanchard, J.; Schüth, F.; Trens, P.; Hudson, M. *Microporous Mesoporous Mater.* **2000**, *39*, 163.
(22) Khushalani, D.; Dag, Ö.; Ozin, G. A.; Kuperman, A. *J. Mater. Chem.* **1999**, *9*, 1491.
(23) Antonelli, D. M. *Microporous Mesoporous Mater.* **1999**, *30*, 315.
(24) Wang, Y.; Tang, X.; Ying, L.; Huang, W.; Rosenfeld Hacohen, Y.; Gedanken, A. *Adv. Mater.* **2000**, *12*, 1183.
(25) Brinker, C. J.; Lu, Y.; Sellinger, A.; Fan, H. *Adv. Mater.* **1999**, *11*, 579.
(26) Yang, P.; Zhao, D.; Margolese, D. I.; Chmelka, B. F.; Stucky, G. D. *Nature* **1998**, *395*, 583.
(27) Yang, P.; Zhao, D.; Margolese, D. I.; Chmelka, B. F.; Stucky, G. D. *Chem. Mater.* **1999**, *11*, 2813.
(28) Soler-Illia, G. J. A. A.; Sanchez, C. *New J. Chem.* **2000**, *24*, 493.
(29) Soler-Illia, G. J. A. A.; Scolan, E.; Louis, A.; Albouy, P. A.; Sanchez, C. *New J. Chem.* **2001**, *25*, 156.
(30) Grosso, D.; Soler-Illia, G. J. A. A.; Babonneau, F.; Sanchez, C.; Albouy, P.-A.; Brunet-Bruneau, A.; Balkenende, A. R. *Adv. Mater.* **2001**, *13*, 1085.
(31) Sanchez, C.; Soler-Illia, G. J. A. A.; Rozes, L.; Caminade, A.-M.; Turrin, C.-O. Majoral, J.-P. *Mater. Res. Soc. Symp. Proc.* **2000**, *628*, CC 6.2.3.
(32) (a) Kriesel, J. W.; Sander, M. S.; Tilley, T. D. *Adv. Mater.* **2001**, *13*, 331. (b) Kriesel, J. W.; Sander, M. S.; Tilley, T. D. *Chem. Mater.* **2001**, *13*, 3554.
(33) Firouzi, A.; Atef, F.; Oertli, A. G.; Stucky, G. D.; Chmelka, B. F. *J. Am. Chem. Soc.* **1997**, *119*, 3596.

The fresh transparent solids are left in Petri dishes or glass plates (1−2 mm thick liquid layers) at $T = 25-70$ °C. The surfaces must be totally flat to avoid segregation of a poorly structured phase upon drying. Translucent glasslike xerogels are obtained upon solvent evaporation. As-synthesized samples were submitted to mild thermal treatment (100−150 °C overnight) to consolidate the inorganic network. Solids were characterized by chemical analysis (Service Central d'Analyse CNRS, Vernaison, France), X-ray diffraction (XRD; Philips PW 1820, graphite-filtered Cu Kα radiation, $\lambda = 1.5406$ Å), Fourier tranformed infrared (FTIR; Nicolet Magna 500, KBr pellets), and transmission electron microscopy (TEM; samples embedded in epoxy resin and ultramicrotomed, JEOL 100 CX II operating at 120 kV). Periodic distances were evaluated from TEM pictures as the average distance between 10 and 15 consecutive maxima; the pore diameter and wall thickness were estimated by considering an intensity below and above 50% of the maximum intensity, respectively.[34]

Thermogravimetric (TGA)/differential scanning calorimetric (DSC) analysis (TA Instruments, SDT 2960) was performed under oxygen or an Ar flux of 100 $cm^3\ min^{-1}$, using a heating ramp of 5 °C $min^{-1}$. Thermal treatment was performed in tubular ovens under a controlled atmosphere. The surface area and porosity of the final oxides was assessed by Brunauer−Emmett−Teller (BET) surface area (Micromeritics ASAP 2010; 60−100 mg samples, ca. 20−30 $m^2$).

## Results and Discussion

**a. Synthetic Approach.** The synthesis method was designed to balance the most important issues previously discussed.[28] Basically, (a) a simple template with an important hydrophilic/lipophilic difference, (b) a polar medium strong enough to allow the development of a mesostructure, (c) a hydrophilic inorganic building block compatible with the polar heads, (d) a method to "turn off" indiscriminate inorganic polymerization before mesostructure formation, and (e) a way to "turn on" extended inorganic polymerization once the mesostructure formed.

CTAB was chosen as the surfactant because of its simplicity, the important solubility difference between the amphiphilic domains, and the absence of a specific interaction with the inorganic precursors. TET was chosen for its relatively moderate reactivity compared to other alkoxides ($Ti(O^iPr)_4$, for example);[35] furthermore, low acid and chloride contents ($p < 2$) can be adjusted in a more controlled way than with $TiCl_4$. A polar solvent is needed to encourage an efficient phase separation. Micelle or mesophase formation is greatly affected by short-chain alcohols (methanol and ethanol) present in sol−gel procedures. These solvents promote an increase of the critical micellar concentration,[36] hindering the organization of mesostructured materials.[37] Therefore, important water quantities were added. The hydrolysis and condensation processes can be efficiently controlled by adding a mineral acid. HCl was added to turn off extended inorganic condensation in the first stages.

The final solutions contain hydrophilic $Ti(OEt)_{4-x-y}Cl_x(OH)_y$ moieties with $x \ll y$ and $x + y \approx 4$, as confirmed by UV/vis.[38] Preferential evaporation of ethanol and HCl raises the pH, while concentrating the solution in water, and the nonvolatile components.[39] Upon this transient pH rise, the titanium species can undergo a partial condensation, generating $TiO_{2-x/2}(OR, OH, Cl)_x$ ($x \approx 0.2-0.5$). Discrete NBB have been characterized in titanium alkoxide/alcohol/acid media by small-angle X-ray scattering (SAXS).[40] In acidic media ($h > 2$), these NBB are compact hydrophilic clusters with a ca. 2 nm gyration radius, depending on pH.[41] Because pH < $pH_{iep\ TiO_2}$, surface hydroxy or $-OH_2^+$ groups are present.[42] Thus, the solid obtained after complete solvent removal should present an $I^+X^-S^+$ type of interface[7] ($X^- = Br^-$ and/or $Cl^-$).

**Table 2. Titania/CTAB Mesophases Obtained by EISA[a]**

| condition | $T$ (°C) | mesophase | $s$ | $p$ | $h$ | [EtOH]/[Ti] |
|---|---|---|---|---|---|---|
| Ti-A-850 | 50 | none | 0.08 | 1.4 | 17 | 20 |
| Ti-A-870 | 70 | WL | 0.08 | 1.4 | 17 | 20 |
| Ti-A-1250 | 50 | WL | 0.12 | 1.4 | 17 | 20 |
| Ti-A-1270 | 70 | WL + H | 0.12 | 1.4 | 17 | 20 |
| Ti-A-1625 | 25 | none | 0.16 | 1.4 | 17 | 20 |
| Ti-A-1650 | 50 | H | 0.16 | 1.4 | 17 | 20 |
| Ti-A-1670 | 70 | H | 0.16 | 1.4 | 17 | 20 |
| Ti-A-2050 | 50 | WL + H | 0.20 | 1.4 | 17 | 20 |
| Ti-A-2070 | 70 | H | 0.20 | 1.4 | 17 | 20 |
| Ti-A-3050 | 50 | WL | 0.30 | 1.4 | 17 | 20 |
| Ti-A-4050 | 50 | WL | 0.40 | 1.4 | 17 | 20 |
| Ti-B-45-5-50 | 50 | H | 0.2 | 5 | 45 | 70 |
| Ti-B-45-5-70 | 70 | WL | 0.2 | 5 | 45 | 70 |
| Ti-B-90-10-50 | 50 | H | 0.2 | 10 | 90 | 70 |
| Ti-B-90-5-50 | 50 | WL | 0.2 | 5 | 90 | 70 |
| Ti-B-90-1.4-50 | 50 | none | 0.2 | 1.4 | 90 | 70 |
| Ti-B-90-10-70 | 70 | WL + H | 0.2 | 10 | 90 | 70 |

[a] WL = wormlike. H = 2D hexagonal (p6m). $s$ = [CTAB]/[Ti]; $h$ = $[H_2O]$/[Ti]; $p$ = [HCl]/[Ti].

**b. Hybrid Phases.** *Structural Characterization*. Systems belonging to Ti-A conditions will be labeled Ti-A-100$sT$; for example, Ti-A-1650 notes the solid synthesized under Ti-A conditions, with $s = 0.16$ at 50 °C (Tables 1 and 2). The mild treatment phases will be denoted Ti-A-100$sT$-100 or Ti-A-$sT$-150, depending on the posttreatment temperature. "Dilute" conditions are indicated as Ti−B-$hpT$. The initial solutions are stable at 298 K for 2−10 days. The hybrid solids have the aspect of a xerogel thick layer and present a grayish-green birefringence under crossed polarizers; this has been observed in thick silica hexagonal films grown on mica under static conditions.[43] SEM analysis shows that

(34) All treatment was performed using IMAGE for Windows analysis software, by D. Petermann, Université de Paris-Sud.

(35) Brinker, C. J.; Scherer, G. W. *Sol−Gel Science*; Academic Press: San Diego, 1990.

(36) Zana, R. *Adv. Colloid Interface Sci.* **1995**, *57*, 1.

(37) Anderson, M. T.; Martin, J. E.; Odinek, J. G.; Newcomer, P. P. *Chem. Mater.* **1998**, *10*, 1490.

(38) $TiCl_4$ was dissolved in ethanol, generating $Ti(OEt)_2Cl_2$ and two HCl molecules (see, e.g., Bradley, D. C.; Merohtra, R. C.; Gaur, D. P. *Metal Alkoxides*; Academic Press: London, 1978). The intensity of the 390 nm band, attributable to chloride complexation, decreases upon water addition. When $h = 10$, this band almost disappears. A similar behaviour was found when adding HCl to alcoholic TET solutions.

(39) Under our synthesis conditions, the initial evaporation of HCl leads to an increase of pH. Subsequent massive departure of ethanol concentrates the solution in water and, to some extent, also in HCl (the HCl/water system presents an azeotropic mixture at $x_{HCl} = 0.2$ and $T_b = 108$ °C; *Handbook of Chemistry and Physics*, 64th ed.; Weast, R. C., Ed.; CRC Press: Boca Raton, FL, 1983−84). In the majority of our systems, HCl is eliminated completely upon a posttreatment. The synthesis media, as well as the final xerogels, present pH < 1; extended condensation of the inorganic network should take place after the complete drying of the final gel (it must be stressed, however, that the ternary HCl/ethanol/$H_2O$ system is far more complicated, and these complications, as well as those stemming from the additional metallic ions, etc., are not taken into account in this first-order discussion).

(40) Kallala, M.; Sanchez, C.; Cabane, B. *Phys. Rev. E* **1993**, *48*, 3692.

(41) Blanchard, J.; Ribot, F.; Sanchez, C.; Bellot, P.-V. Trokiner, A. *J. Non-Cryst. Solids* **2000**, *265*, 83.

(42) Yoon, R. H.; Salman, T.; Donnay, G. *J. Colloid Interface Sci.* **1979**, *70*, 483.

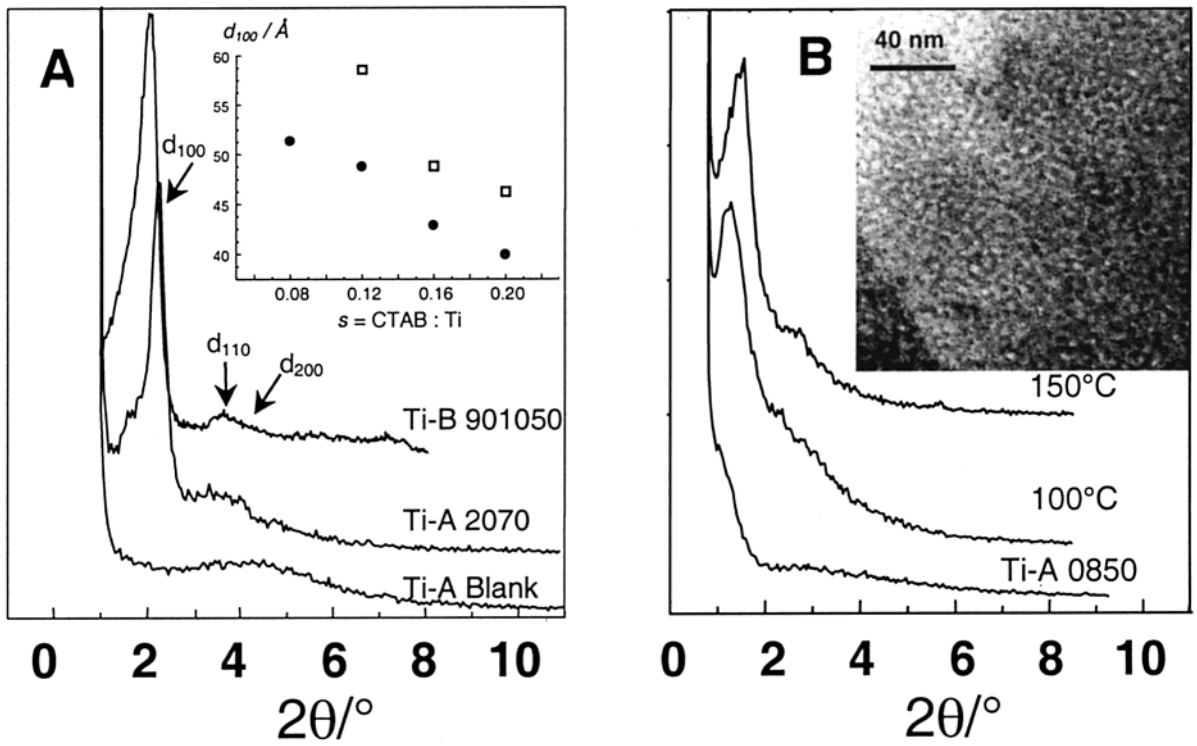


**Figure 1.** Low-angle powder XRD patterns of as-prepared Ti/CTAB hybrids under Ti-A and Ti-B conditions (A; see Table 1 for abbreviations); the inset shows the variation of the $d_{100}$ distance of Ti-A-*sT* systems with the CTAB contents ($s$ = [CTAB]/[Ti]) at 50 °C (open squares) and 70 °C (full circles). (B) Powder XRD of Ti-A-0850 hybrids, as prepared and submitted to mild thermal treatment overnight. Inset: TEM micrograph of a wormlike solid obtained after 150 °C (Ti-A-0850−150).

the resulting xerogels are smooth to the micrometer scale, with the typical thickness being 200−500 $\mu$m.

Different textural and mesostructural characteristics are obtained, depending on $h$, $p$, $s$, and $T$, as depicted in Figure 1A. For Ti-A systems with $s = 0.12-0.20$, XRD patterns display a sharp peak at low angles (40−55 Å; see the inset), corresponding to an ordered structure, and other less defined peaks in the 15−25 Å zone. Samples with $s < 0.1$ or $s > 0.2$ present less sharp XRD peaks, depending on the temperature (see below). This pattern corresponds to less ordered mesostructures (wormlike or local hexagonal).

The peaks in the 15−25 Å zone are superimposed to a hump at ca. 20−25 Å, which is present in all as-prepared materials, even in a "blank" xerogel with no surfactant (Figure 1A); a similar phenomenon has been reported in block copolymer templated titania.[28] This is in agreement with classical studies on Ti-oxo gels, where randomly arranged spheroidal amorphous titania particles originate a texture at the 30 Å scale.[44] This is coherent with the outlined NBB approach: in the present synthesis conditions, discrete hydrophilic nanosized Ti-oxo NBB are formed prior to the development of a mesostructured hybrid phase.[28,40,41]

*Surfactant Effect.* The inset in Figure 1A shows the variation of $d_{100}$ with temperature and $s$ for Ti-A systems. The values of $d_{100}$ are in agreement with previously reported data on Ti−CTAB-based hybrid materials.[18−22] $d_{100}$ diminishes with increasing $s$; this effect is inherent to the synthesis method. For constant Ti, EtOH, and HCl/water concentrations, the increasing concentration of CTAB in the final gel leads to a smaller intermicelle separation. The same phenomenon has been found in water/CTAB systems (or $H_2O$/CTAB/EtOH) presenting a bidimensional hexagonal structure. The cell parameter decreases from 75 to 54 Å when the surfactant contents is increased from 33 to 64% by mass; however, the diameter of the rodlike aggregate (micelle) is kept approximately constant.[45] This has been linked to the conservation of the area per polar group: if more micelles have to be created, the intermicellar space should be sacrificed. This is also valid for a disordered sample; addition of CTAB increases the extent of the hybrid interface (the "interface contents"); thus, the wall thickness must decrease.

*Temperature Effects.* The effects of temperature are not straightforward because a variety of factors are involved, and this parameter is thermodynamic and kinetically relevant. It has been reproducibly observed that $d_{100}$ decreases with increasing temperature. This can be discussed on the basis of two competing processes: solvent evaporation and condensation of the inorganic network, both depending on $T$. At 50 °C, Ti-A samples with $s > 0.1$ yield directly an organized mesophase. At 60−70 °C, ordered hybrid mesophases are produced in all cases. Higher temperature leads to a more complete removal of solvent, which explains the lower periodical distances found at 70 °C, and also a more extended condensation degree of the inorganic network (see the next section).

Temperature also plays a decisive kinetic role by affecting the dynamical interplay of evaporation and

(43) Yang, H.; Coombs, N.; Ozin, G. A. *J. Mater. Chem.* **1998**, *8*, 1205.

(44) Wright, A. F.; Mukherjee, S. P.; Epperson, J. E. *J. Physique (France)* **1985**, *46*, C8−521.

(45) Fontell, K.; Khan, A.; Lindström, B.; Maciejewska, D.; Puang-Ngern, S. *Colloid. Polym. Sci.* **1991**, *269*, 727.

condensation rates. The first effect to consider is an increase of the solvent evaporation rate, leading to a faster formation of the liquid-crystal mesophase. In general, Ti-A systems are better organized at 70 °C. Organization does not take place when evaporating at ambient temperature, and dilution of the starting solutions with ethanol (i.e., longer evaporation time) results in less defined mesostructures. These results indicate that the quick formation of a concentrated liquid-crystal phase favors ordering. When solvent is slowly removed, a relatively quick and extended co-condensation of the preformed NBB traps the template molecules (and not any micellar aggregates) in an amorphous matrix. This is clearly seen in the 50 °C systems: an increase in *s* leads to an ordered mesostructure. Increasing the temperature also increases the condensation rate of the inorganic framework. An adequate balance between both processes (solvent evaporation versus inorganic condensation) is necessary to attain the desired segregation of micellarlike species at the mesoscale.

In Ti-B systems (Table 2), the best organization is attained at 50−60 °C. In these water-rich and dilute systems, the temperature effect on condensation takes over the enhanced evaporation rate. The fast formation of an extended gel leads to less defined mesophases presenting higher order distances. However, for low temperatures and high inhibition rates (50 °C, $p = 10$), Ti-B systems present a remarkable degree of order (Figure 1A).

*Postprocessing Effect*. Prolonged treatment at 60−80 °C helps to eliminate excess HCl and improve condensation and the definition of the mesophase; the *a* parameter decreases slightly (less than 5%). Accordingly, a small segregation of CTAB is observed, in agreement with a dynamic hybrid structure. Phase transitions upon thermal treatment have already been reported in mesostructured silica and non-silica suspensions,[8,46] where the solution acts as a vehicle for the transformation. These rearrangements can also be achieved by prolonged treatment under vacuum.[43]

For example, Ti-A-0850 hybrids do not display order; however, when treated at 100−150 °C overnight, XRD ordering peaks show up (Figure 1B, inset). This strongly suggests that the condensation of the inorganic framework in the as-prepared samples is not complete. A "titaniatropic" hybrid assembly is formed, where the extended condensation process is decoupled from the organization, as in silicatropic systems.[33] For EISA-based film synthesis, these transitions[25,47] are known to occur even in the absence of solvent because of the liquid-crystalline nature of the as-prepared mesostructures.

*TEM Studies.* TEM images of the different hybrid phases obtained are shown in Figure 2. When $s \leq 0.12$, coexisting wormlike and hexagonal domains are observed. For $0.12 < s < 0.30$, hexagonal and local hexagonal (quasi-hexagonal) domains can coexist; the optimal conditions for an ordered two-dimensional hexagonal phase (p6m), presenting well-defined and extended domains (Figure 2 a−c) are situated between 0.15 and 0.20. When $s > 0.3$, domains seem to be composed of coated 2−3 nm entities rather than channels surrounded by inorganic walls; i.e., there seems to be a change in the curvature (Figure 2d).

The $d_{100}$ distances agree well with those found by XRD, being systematically lower in the case of the hybrids (ca. 10% for Ti-A-1650, 44 ± 4 Å (TEM) vs 48 ± 2 Å, respectively); this can be attributed to a partial shrinkage and decomposition of the sample under the electron beam.[21] The lamellar-like regions observed are due to a projection of a hexagonally packed array of tubes.[48] The wall thickness has been estimated as 20 ± 2 Å. This value is high if compared to that reported for MCM-41, 8 ± 1 Å,[1,49] or TM oxophosphates (ca. 10−12 Å[50]). The size of the "organic cavities" in the initial hybrids is estimated as 25−30 Å for Ti-A-1650, for a total interpore distance of 45−50 Å (corresponding to $d_{100}/(3/2)^{1/2}$).

**c. Hybrid Phases.** *Macroscopic and Chemical Characterization*. The solubility of mesostructured titania xerogels strongly depends on the synthesis temperature. While Ti-A-*s*50 is soluble in water, the mesostructure of Ti-A-*s*70 is kept after resuspension in water or ethanol. A mild thermal treatment of any Ti-A-*s*50 hybrid at 100−150 °C suffices to render this hybrid insoluble in water. This supports the statement of the previous section: the inorganic walls of the initial mesophase are formed by loosely bound inorganic NBB. These primary building units must be linked together by further polymerization to generate a robust mesophase. This has also been observed for "dry-consolidated" wormlike titania.[23]

Chemical analyses of as-synthesized and treated hybrids (Table 3) show that the global composition of these solids is $TiO_{2-x/2-z}(OH)_z(CTA^+)_s(Br, Cl)_{s+x+z}(H_2O)_y$; typically, $x < 0.3$, $y < 0.1$, and the water content is about 10% by mass, according to TGA (see below). Halogenide ions are compensating the charge of the $CTA^+$ ions, and minor quantities of protons are associated with surface $\equiv Ti-OH_2^+$ or $Ti-OH^+$ groups.[51] Some of the chloride anions can be coordinated to Ti, substituting ethanol or ethoxy groups; interestingly, the latter are practically absent (C:N ratio ≈ 19), which has been confirmed by FTIR (see below). Upon thermal treatment to 100 °C overnight, a weight loss of 10−15% is recorded; the systems lose water, chloride, and bromide. At 150 °C, the weight loss is slightly higher; in this stage, a slight decomposition of the surfactant can be observed (C:N < 19 and N:Ti < *s*).

Four main zones can be distinguished in the FTIR spectra (Figure 3). (a) 4000−3000 $cm^{-1}$ ($\nu_{OH}$): as-prepared samples display a composite absorption (3400 $cm^{-1}$ and large 3000−3350 $cm^{-1}$), attributable respectively to structure or surface hydroxyl groups (including strongly bound water) and OH groups from adsorbed solvent (ethanol and water);[35,52] the latter band is less

(46) Neeraj, S.; Rao, N.; Rao, C. N. R. *J. Mater. Chem.* **1998**, *8*, 1631.
(47) Kundu, D.; Zhou, H. S.; Honma, I. *J. Mater. Sci. Lett.* **1998**, *17*, 2089.
(48) Chenite, A.; Le Page, Y.; Sayari, A. *Chem. Mater.* **1995**, *7*, 1015.
(49) Behrens, P.; Glaue, A.; Haggenmüller, C.; Schechner, G. *Solid State Ionics* **1997**, *101−103*, 255.
(50) Lindén, M.; Blanchard, J.; Schacht, S.; Schunk, S.; Schüth, F. *Chem. Mater.* **1999**, *11*, 3002.
(51) Hiemstra, T.; Van Riemsdijk, W. H.; Bolt, G. H. *J. Colloid Interface Sci.* **1989**, *133*, 91.
(52) Nakamoto, K. *Infrared and Raman Spectra of Inorganic and Coordination Compounds*, 4th ed.; Wiley: New York, 1986.

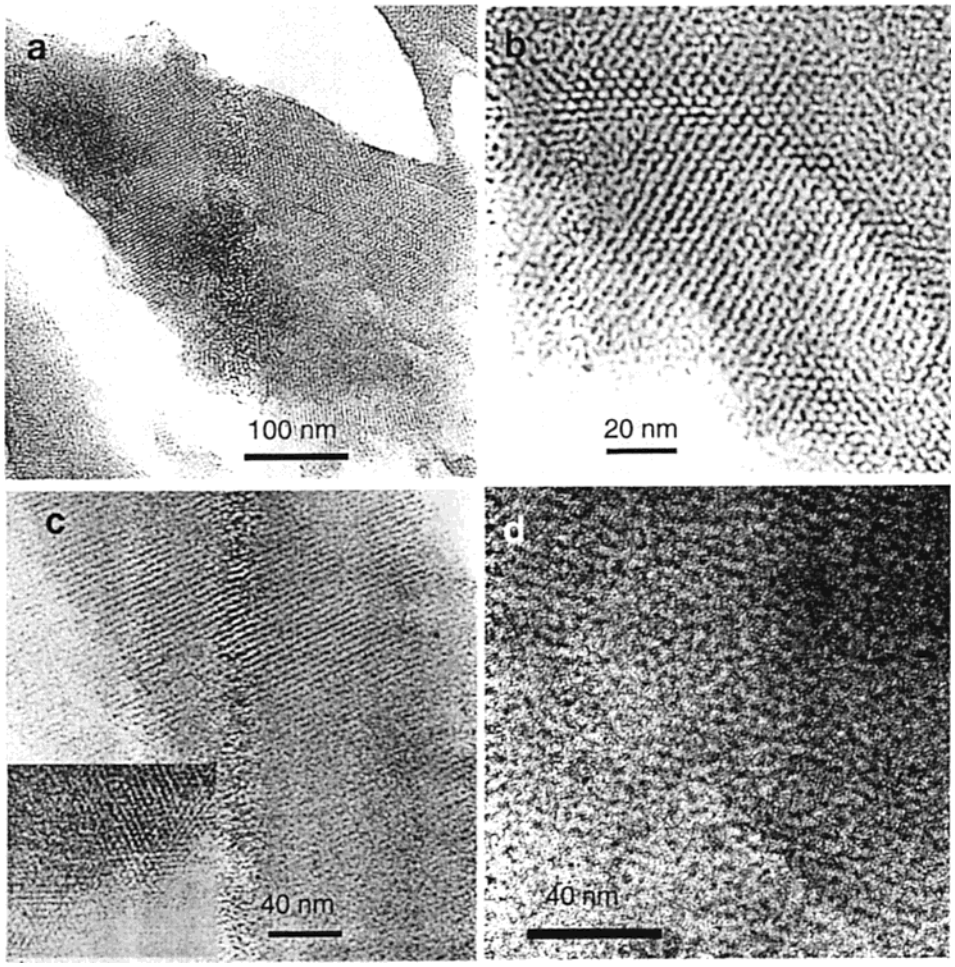


**Figure 2.** TEM micrographs of hybrid $TiO_2$/CTAB samples. As-synthesized Ti-A-1650 (a; detail in b). Ti-A-1650 treated to 150 °C overnight (c), displaying parallel channels (along the *z* axis) and hexagonal domains (inset). (d) Dispersion of amorphous nanometric $TiO_2$ particles obtained in the Ti-A-2550 system.

**Table 3. Chemical Composition of As-Prepared and Treated Ti-A-100*sT* Hybrids**

| | Ti-A-0850 | Ti-A-0850 at 100 °C | Ti-A-1250 | Ti-A-1250 at 100 °C | Ti-A-1270 | Ti-A-1650 | Ti-A-1670 |
|---|---|---|---|---|---|---|---|
| mesostructure[a] | none | WL | WL | WL + H | WL + H | H | H |
| C:N | 21.2 | 14.3 | 19.6 | 13.6 | 19.8 | 19.6 | 21.5 |
| Br:N | 0.91 | 0.47 | 0.95 | 0.62 | 0.90 | 0.85 | 0.78 |
| Cl:N | 3.2 | 1.2 | 3.6 | 1.9 | 2.8 | 1.8 | 1.5 |
| C:Ti | 1.8 | 1.6 | | | | 3.3 | 3.3 |
| N:Ti | 0.08 | 0.11 | | | | 0.17 | 0.15 |
| Cl:Ti | 0.27 | 0.13 | | | | 0.31 | 0.23 |
| Br:Ti | 0.07 | 0.05 | | | | 0.14 | 0.12 |

[a] WL = wormlike. H = 2D hexagonal (p6m).

significant in the samples synthesized at 70 °C; both bands fade (relative to the C−H vibrations) upon mild thermal treatment. (b) 3000−2800 $cm^{-1}$ ($\nu_{CH}$): characteristic bands of template $CH_2$ and $CH_3$ groups. (c) 1700−1000 $cm^{-1}$ ($\delta_{OH}$, $\delta_{CH}$, and $\nu_{CO}$): $\delta_{OH}$ of adsorbed water (1625 $cm^{-1}$); $\delta_{CH}$ vibrations of CTAB are a set of absorptions in the 1500−1350 $cm^{-1}$ region; interestingly, the absence of C−O stretching indicates that no alcohol or alkoxide (from incomplete condensation)[53] is present in the hybrid samples. (d) Low-frequency bands in the range 900−400 $cm^{-1}$ correspond to the $\nu_{TiOTi}$ of the mineral network, evidencing partial condensation in the as-synthesized hybrids. The intensity of this large band is enhanced upon thermal treatment as the cocondensation proceeds.

The preceding results indicate that the nature of the mesostructured hybrids can be described as a "titania-tropic" phase composed of Ti-oxo-based NBB, self-assembled around a lyotropic mesophase.[33] Two interfaces are defined: (a) a hybrid interface of the $I^+X^-S^+$ type, composed of the surfactant, chloride, or bromide ions, and the globally positively charged Ti-oxo NBB and (b) the individual interface of these Ti-oxo NBB, composed of $Ti-OH_2^+$ groups and chloride ions, coordinated or not to Ti surface atoms (Scheme 1).

The presence of hexagonal or wormlike phases can be explained in terms of a disorder to order transition, with the order being triggered by the existence of the air−solution and solution−container interfaces, which exert an important effect on mesophase formation. This

(53) (a) Doeuff, S.; Henry, M.; Sanchez, C.; Livage, J. *J. Non-Cryst. Solids* **1987**, *89*, 206. (b) Doeuff, S.; Dromzee, Y.; Taulelle, F.; Sanchez, C. *Inorg. Chem*. **1989**, *28*, 4439.

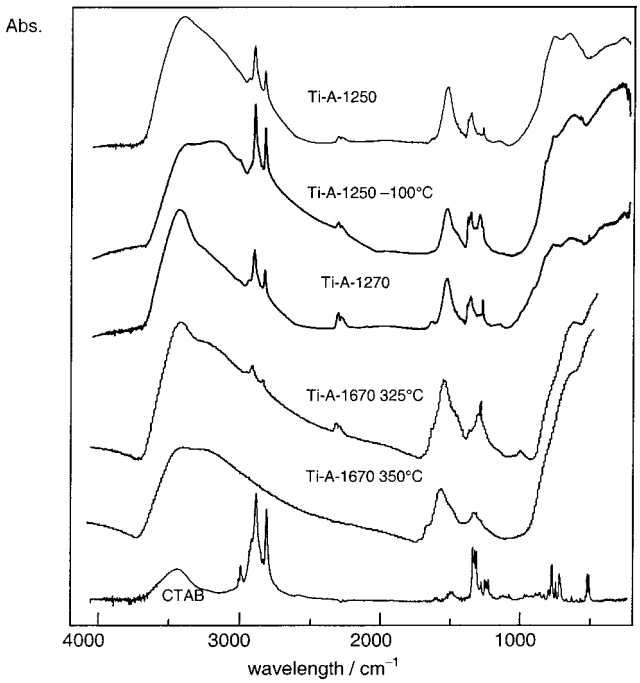


**Figure 3.** FTIR spectra of Ti-A-12*T* hybrids and calcined Ti-A-1650. For abbreviations, please refer to Table 1.

has been thoroughly studied in silica systems obtained in quiescent conditions from dilute aqueous solutions by the groups of Ozin,[43,54] Aksay,[55] and White.[56] Regardless of the differences between these approaches, it is generally agreed that the perturbations induced by the system boundaries play a relevant role. Micellar arrays form spontaneously at both interfaces, triggering the formation of the mesostructures. Recent work on mesostructured silica films has suggested that a disorder to order transition might be responsible for the observed structures.[55] An initial set of disordered channels rearranges into an ordered array of pores. This may take place in some domains where formation of ordered nuclei should be followed by the growth of an extended organized mesophase. A general description proposed that entities (particles or gel environments) can "begin as disordered silicate−surfactant assemblies which mesoscopically crystallize after some induction period".[55] In the systems presented here, the first assemblies that appear upon evaporation can be expected to be disordered because the template concentration is not high enough to permit the construction of a well-defined hybrid interface by self-assembly of the micelles and the NBB. This is clear from the Ti-A experiments in the lower surfactant region, which show the evolution from a wormlike disordered mesophase to an ordered hexagonal arrangement. We have also observed this wormlike to hexagonal phase transition in the formation of $TiO_2$/Pluronic mesostructured thin films by in situ SAXS.[57] Upon solvent evaporation, the initial NBBs can interact with each other or with the surfactant, because they are "squeezed" together by the contraction of the reaction volume, and the order advances throughout the sample.[55] Once the final volume is reached and the liquid-crystal phase is kinetically "frozen", the systems are able to reorganize, to optimize the ionic, colloidal, and van der Waals interactions between the inorganic NBB and the micelles. However, this reorganization is activated, as demonstrated in Figure 1B. The range $s = 0.15-0.2$ seems to be the optimal one to obtain a p6m organization before solvent evaporation "freezes" a less organized mesostructure. An excess of template with respect to Ti-oxo NBB can invert the situation, and the resulting structure will be rather an array of amorphous $TiO_2$ NBB surrounded by surfactant molecules, resembling reverse micellar systems (Scheme 1).[58]

**d. Thermal Analysis.** Figure 4 shows TGA and DSC traces for Ti-A-1650; the curves are similar to those previously reported for mesostructured materials.[1,7,59,60] By careful comparison of the thermal losses in samples with variable *s* or treatment (Figure 5), the path from the hybrid precursor to the final oxide can be divided into four steps: below 100 °C, 100−210 °C, 210−330 °C, and greater than 330 °C.

When the thermal loss is crossed with FTIR and chemical analysis, the four stages can be described as follows: (a) Below 100 °C, 9−13% mass loss is due to volatile species (water, ethanol, and/or HCl, as assessed by elemental analysis). This is coincident with the decrease in the $\nu_{OH}$ absorption upon mild thermal treatment (Figure 3). (b) From 100 to 210 °C, a mass loss of 5−10% is associated with a slightly exothermic process. In samples that have been thermally treated (100−150 °C), this mass loss decreases significantly (Figure 5A), as does the $Cl^-$ content, which decreases monotonically with temperature (less than 20 ppm chloride is present after 220 °C). This can be attributed to the liberation of water, HCl, or organochloro compounds.[61] This suggests that in this step condensation of residual hydroxyl groups "inter-NBB" proceeds, ensuring a more condensed and compact inorganic network. A minor degradation of the template is also detected. (c) The mass loss of the third step is in all cases lower than the mass of CTAB and does not depend on the previous "mild" thermal treatment (Figure 5A); conversely, a strong dependence on *s* is evident (Figure 5B). This can be attributed to partial surfactant decomposition, which seems to occur in two successive steps, corresponding to linked exothermic processes taking place at ca. 250 °C (Figure 4, step c) and 280 °C (Figure 4, step c′). These two steps might correspond to the cleavage of the $CTA^+$ cations and the subsequent oxidation of the organic template backbone, as has been reported in detail in MCM-41[1,59] and mesostructured Ti-oxophosphates.[60] However, some residual organic matter is still present, as amorphous carbon (the samples are brown/black) or carboxylate species linked

(54) Yang, H.; Coombs, N.; Sokolov, I.; Ozin, G. A. *J. Mater. Chem.* **1997**, *7*, 1285.
(55) Yao, N.; Ku, A. Y.; Nakagawa, N.; Lee, T.; Saville, D. A.; Aksay, I. A. *Chem. Mater.* **2000**, *12*, 1536 and references therein.
(56) Ruggles, J. L.; Holt, S. A.; Reynolds, P. A.; White, J. M. *Langmuir* **2000**, *16*, 4613.
(57) Crepaldi, E. L.; Soler-Illia, G. J. A. A.; Grosso, D.; Albouy, P.-A.; Amenitsch, H.; Sanchez, C. *Proceedings of Nanoporous Materials III*, to be held in Ottawa on June 12-15, 2002, in press.
(58) Kluson, P.; Kacer, P.; Cajthaml, T.; Kalaji, M. *J. Mater. Chem.* **2001**, *11*, 644.
(59) Keene, M. T. J.; Gougeon, R. D. M.; Denoyel, R.; Harris, R. K.; Rouquerol, J.; Llewelyn, P. L. *J. Mater. Chem.* **1999**, *9*, 2843.
(60) Kleitz, F.; Schmidt, W.; Schüth, F. *Microporous Mesoporous Mater.* **2001**, *44−45*, 95.
(61) Poncelet, O.; Guilment, J.; Truchet, S. *Mater. Res. Soc. Symp. Proc.* **1994**, *346*, 655.

**Scheme 1. Idealized Formation Pathway of $TiO_2$/CTAB Hybrids**[a]

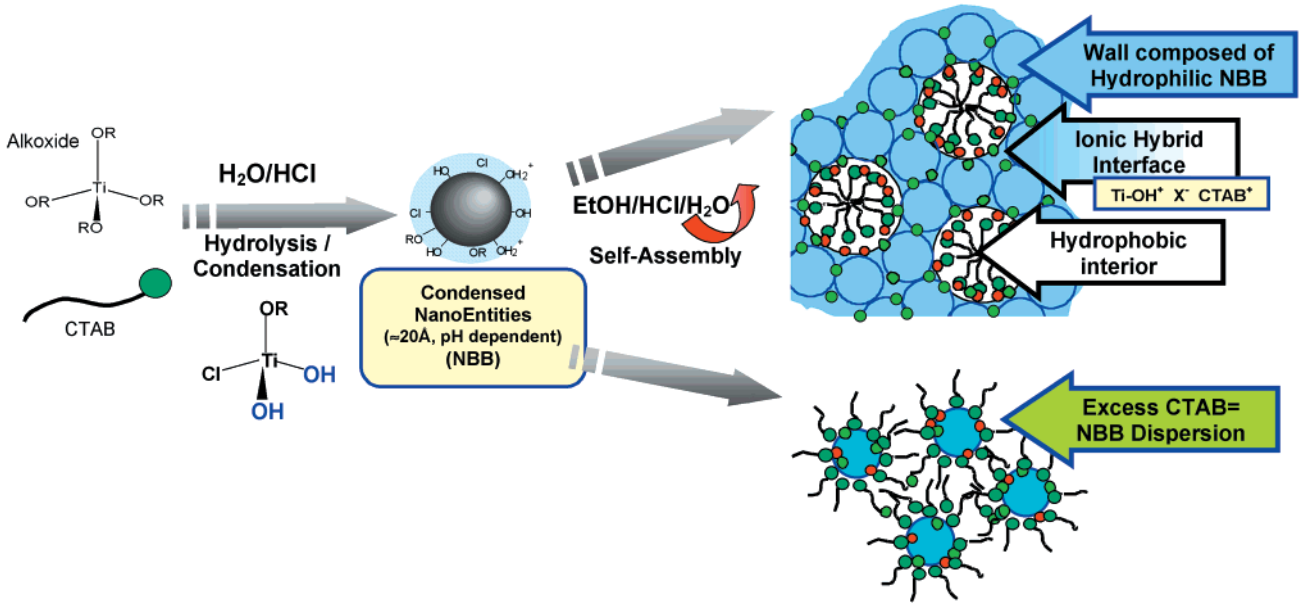


[a] Hydrolysis leads to a distribution of Ti-hydroxochloroalkoxo species, which can condense upon departure of HCl. Colloidal Ti-oxo entities (nanobuilding blocks, NBB) result from partial condensation. These units present a charged surface due to ≡Ti−OH and ≡Ti−$OH_2^+$ groups. Further evaporation of the solvent enables the formation of a liquid-crystalline phase, formed by an assembly of precondensed Ti-oxo entities around tubular micelles built by self-assembled amphiphilic molecules. The cohesion of these superassemblies is ensured by anions (chloride, in green; bromide, in red) that counterbalance the charges of CTAB and the positively charged NBB. The whole structure is relatively fragile and has to be further linked by cocondensation between the NBB. An excess CTAB gives rise to an inversion of the curvature, and dispersions of NBB are observed.

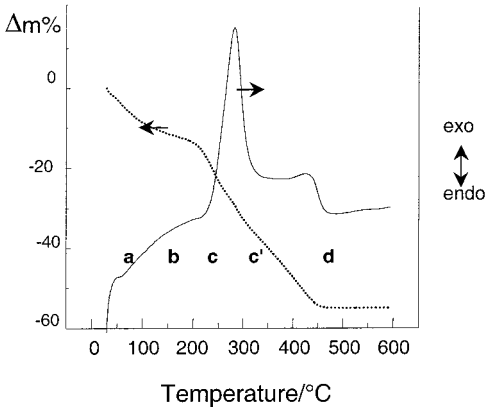


**Figure 4.** TGA and DSC curves belonging to a Ti-A-1650 hybrid. The five marked temperature zones are discussed in the text.

to the titania framework, as evidenced by FTIR (1543 and 1400 $cm^{-1}$; Figure 3). These species are completely eliminated at $T > 330$ °C. (step d). Water loss due to a total dehydration can also take place at these temperatures. Oxidation of the residual organic components is followed by extended crystallization to anatase ($T >$ 400 °C).

XRD patterns recorded for a Ti-A-2070 sample heated successively (during periods of 30 min) to 400 °C show a progressive broadening and shifting of $d_{100}$ to lower distances. The contraction, $d_0 - d/d_0$ ($d_0 = d_{100}$ for the fresh hybrid), is below 5% for $T < 200$ °C; above 200 °C, it is in the 20−23% range, coinciding with a decay of the diffracted intensity (Figure 6, inset). Partial degradation of the structure goes along with surfactant decomposition. By 400 °C, anatase crystallization occurs, which destroys the mesostructure.

**e. Thermal Treatment and High Surface Area Porous $TiO_2$.** Calcination of hybrid samples in a controlled atmosphere leads to high surface area titania, presenting pores in the limit of micro- and mesoporosity. Two limitations arise in the thermal treatment step. The first one is imposed by the massive formation of anatase at 400 °C. In addition, a low heating rate is needed to avoid a sudden contraction and to separate the exothermic events, two factors that deteriorate the mesostructure. Samples were thus heat-treated using a slow ramp (1.5 °C $min^{-1}$) up to 120 °C under argon, followed by a temperature ramp of 0.5 °C $min^{-1}$ up to 350−400 °C under an oxygen or air atmosphere; the final temperature is kept for 2−70 h to eliminate the organics. XRD patterns (Figure 6A) show that the mesoscale order is kept until a 4 h treatment at 350 °C. The $d_{100}$ parameter shifts to 34−37 Å for typical systems, and the hexagonal domains are conserved, as shown in Figure 6B; the pore size and the wall thickness can be estimated from TEM in 22 and 18 Å, respectively (Figure 6C). At the same time, a low signal corresponding to anatase nanodomains (3−4 nm according to the Scherrer equation) is detected by high-angle XRD. This crystalline fraction can be observed in some of the TEM pictures as bright, dense spots (particles) associated with the mesostructured domains. In previous work with PEO-based surfactants, Yang et al.[27] found that these crystalline domains were embedded in the mostly amorphous titania matrix; similar results have been obtained in our laboratory for mesostructured bulks or films.[62] In PEO-templated systems, the walls are thicker (ca. 40 Å) than those in the CTAB case, which allows nanocrystalline walls to be produced. Cabrera et al. also reported 3 nm

(62) Sanchez, C.; Soler-Illia, G. J. A. A., unpublished work.

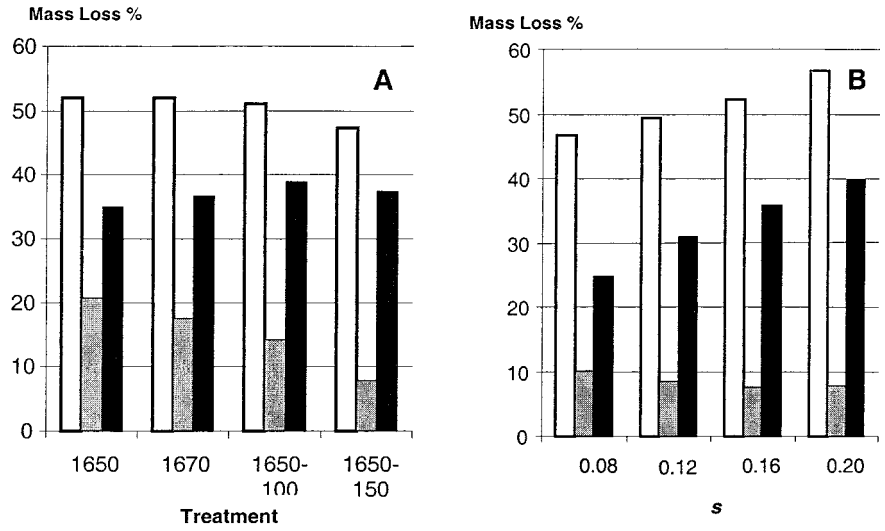


**Figure 5.** TGA mass loss for Ti-A samples with constant composition ($s = 0.16$) and different previous thermal treatment (A) or different composition, synthesized at 50 °C (B). Bars represent the total mass loss (white), 100−200 °C (gray), and 220−450 °C (black).

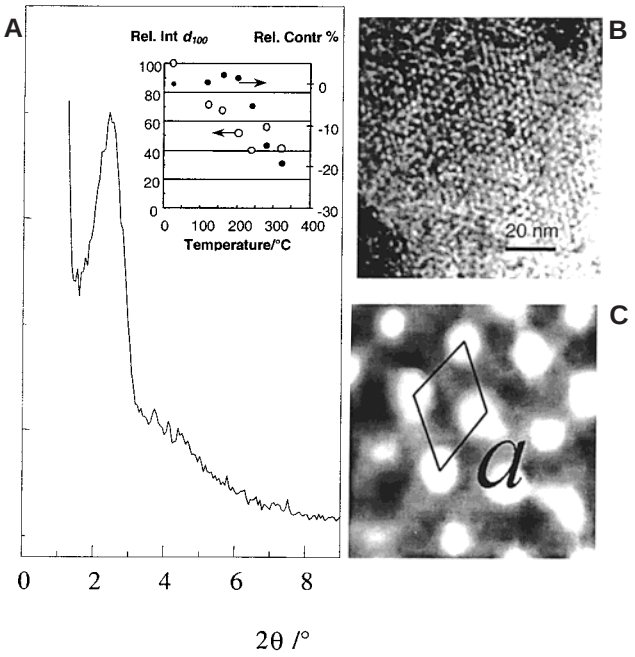


**Figure 6.** (A) XRD pattern of Ti-A-1650 (a) and -2070 (b) samples calcined at 350 °C for 4 h. Inset: relative intensity (open circles) and relative contraction (closed circles) of the $d_{100}$ line for Ti-A-2070 upon heating (20 min intervals at each temperature). (B) TEM picture of a Ti-A-1550 sample thermally treated at 350 °C for 4 h. (C) Detail (10×) of B; the walls of the mesopores cover approximately half of the interpore distance.

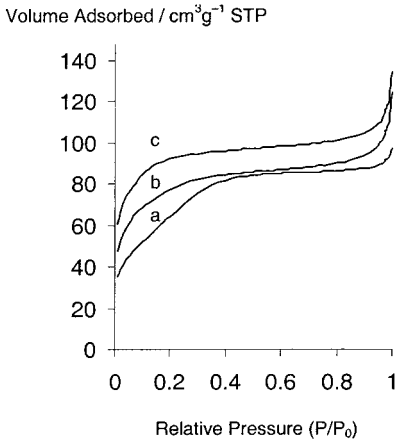


**Figure 7.** $N_2$ adsorption isotherms of Ti-A-1670 submitted to different thermal treatments: (a) 300 °C, 70 h; air atmosphere. (b) 325 °C, 8 h; $Ar/O_2$ atmosphere. (c) 350 °C, 4 h; $Ar/O_2$ atmosphere. Only adsorption isotherms are shown. Refer to the text for detailed treatments and to Table 3 for the adsorption characteristics.

anatase in the mesoporous walls of a wormlike material.[17] In the presented CTAB-templated titania, it is not clear whether these nanocrystals are embedded into the mesostructure (with their mean size being larger than the wall thickness), are stuck to the walls, or are a result of a partial "explosion" of the channel structure. At $T > 350$ °C or higher heating time, the anatase nuclei begin to grow extensively and segregate from the mesostructures. Subsequently, the whole mesostructure is completely destroyed.

Figure 7 depicts typical $N_2$ adsorption−desorption isotherms for calcined Ti-A-1670, submitted to different conditions. The aspects of the isotherm, surface area, and porous volume estimated by BET (Table 4) are dependent on the final temperature and heating time. For example, the adsorption isotherm of a Ti-A-1670 sample calcined to 300 °C shows a slight break at $P/P_0 = 0.2$, and the associated surface area is 235 $m^2\ g^{-1}$. FTIR spectra of samples in this stage show that not all of the organic component is removed (Figure 3). Further thermal treatment is needed to eliminate the template completely, which results in an enhancement of the surface area and the porous volume; this leads to the development of microporosity. The values of surface area, pore volume, and pore size (estimated by BET single point $P/P_0 = 0.994$) are only indicative, and no significant differences can be extracted from the reported data. Globally, the pores are in the 20−25 Å range and the wall thickness is in the 20 Å, as was measured from TEM images (Figure 6C).

It should be recalled that the BET model used is not completely suitable for pores in the micropore−mesopore range and BET measurements tend to overestimate surface areas.[63] Alternative analysis methods (for

**Table 4. XRD and BET Parameters of Calcined $TiO_2$ Samples Obtained from Ti-A Hybrids**

| sample | calcination temp (°C) | calcination time (h) | BET surface area ($m^2\ g^{-1}$) | $V_p$ ($cm^3\ g^{-1}$) | pore diameter (Å)[a] | wall thickness (Å)[b] | XRD $d_{100}$ (Å) |
|---|---|---|---|---|---|---|---|
| blank | 325 | 8 | <30 | 0.02 | | | |
| 1550 | 350 | 4 | 370 | 0.19 | 20 | 22, 21 (TEM) | 37 |
| 1670 | 325 | 8 | 266 | 0.17 | 25 | 15 | 36 |
| 1670 | 350 | 4 | 360 | 0.19 | 24 | 16 | 35 |
| 2070 | 350 | 1 | 284 | 0.16 | 21 | 18 | 34 |
| 2070 | 350 | 4 | 324 | 0.16 | 19 | 20 | 34 |

[a] Estimated by BET as 4 V/A. [b] Estimated as the interpore distance−pore diameter.

example, density functional theory) should give a better result.[21,64] However, these estimations allow for comparison with previous work; the surface area and pore size are in the same range.[65] Yet, the aspect of the isotherms resembles that of a microporous molecular sieve rather than an MCM-41 material for the materials calcined at high temperature. This feature has been reported in many papers along with the titania/CTAB literature[13,21,23] and may be due to partial blocking of the channels by residual carbonaceous material,[60] therefore reducing the mean pore size and hindering capillary condensation. According to the shape of the isotherms, micropores are liberated upon further calcination. Organic material resulting from incomplete decomposition of CTAB can be partially deposited on the pore walls. Microporosity can also arise from the liberation of this organic layer, exposing the walls that should be microporous, as a consequence of being formed by NBB.

## Conclusions

EISA is a valid alternative to the reproducible synthesis of mesostructured phosphate and sulfate-free titanium oxide based hybrid mesophases. Simple synthesis concepts can be developed, which are illustrated in this work: the complex interrelation between the fundamental synthesis variables such as concentration, *h*, *p*, *s*, and temperature have been partially elucidated, permitting the design of TM-based mesostructured materials.

Upon evaporation, hydrophilic Ti-oxo nanospecies are formed, which act as primary NBB of the inorganic walls. The initial acidic media hinders condensation between these NBB, which, in the presence of CTAB and during solvent evaporation, lead to a hybrid "titaniatropic" phase. The organization mode of these hybrid phases depends on the surfactant-to-titanium ratio. At low CTAB content, the surfactant molecules cannot act with sufficient cooperativity to be able to impose enough curvature to the Ti-oxo growing polymers, and therefore wormlike hybrid phases are obtained. For intermediate surfactant-to-titania ratios, these mesostructures are organized into hexagonal networks, while for higher CTAB/Ti ratios, inverse micelles having Ti-oxo cores are obtained. Titania phases obtained through a careful thermal treatment are stable up to 350 °C; they present mesoorganization, high surface area (370 $m^2\ g^{-1}$), and pores ranging in the meso/micropore scale. These materials are going to be tested for photocatalysis, and therefore the present work is currently being extended to seek alternative methods to optimize the surfactant removal and the crystallinity of the titania walls while keeping the high mesostructured surface areas already obtained.

**Acknowledgment.** Authors are indebted to the eternal M. Lavergne for the TEM images and to CNRS and UPMC for general funding. G.J.A.A.S.-I. acknowledges financial support from CONICET and Fundación Antorchas.

CM011217A

(63) Kruk, M.; Jaroniec, M.; Sayari, A. *Langmuir* **1997**, *13*, 6267.
(64) Sonwane, C. G.; Bhatia, S. K. *J. Phys. Chem. B* **2000**, *104*, 9099.

(65) Typical values for mesoporous $TiO_2$ obtained by thermal treatment: Antonelli and Ying (200 $m^2\ g^{-1}$, 32 Å), Stone and Davis (300 $m^2\ g^{-1}$, 24 Å), Blanchard et al. (340 $m^2\ g^{-1}$, 21 Å), and Trong On (310 $m^2\ g^{-1}$, 36 Å).